

This article was downloaded by:

On: 18 January 2011

Access details: *Access Details: Free Access*

Publisher *Taylor & Francis*

Informa Ltd Registered in England and Wales Registered Number: 1072954 Registered office: Mortimer House, 37-41 Mortimer Street, London W1T 3JH, UK



International Journal of Polymeric Materials

Publication details, including instructions for authors and subscription information:

<http://www.informaworld.com/smpp/title~content=t713647664>

Microstructural Development of Uniaxial Stretched Anneal-Oriented Syndiotactic Polystyrene and its Blend with Poly (2,6-dimethyl-1,4-phenylene oxide): DSC, WAXD, SAXS and FTIR Studies

Asok Kumar Dikshit^a

^a Central Glass and Ceramic Research Institute (CGCRI), Kolkata, India

Online publication date: 29 June 2010

To cite this Article Dikshit, Asok Kumar(2010) 'Microstructural Development of Uniaxial Stretched Anneal-Oriented Syndiotactic Polystyrene and its Blend with Poly (2,6-dimethyl-1,4-phenylene oxide): DSC, WAXD, SAXS and FTIR Studies', *International Journal of Polymeric Materials*, 59: 8, 628 – 645

To link to this Article: DOI: 10.1080/00914031003760741

URL: <http://dx.doi.org/10.1080/00914031003760741>

PLEASE SCROLL DOWN FOR ARTICLE

Full terms and conditions of use: <http://www.informaworld.com/terms-and-conditions-of-access.pdf>

This article may be used for research, teaching and private study purposes. Any substantial or systematic reproduction, re-distribution, re-selling, loan or sub-licensing, systematic supply or distribution in any form to anyone is expressly forbidden.

The publisher does not give any warranty express or implied or make any representation that the contents will be complete or accurate or up to date. The accuracy of any instructions, formulae and drug doses should be independently verified with primary sources. The publisher shall not be liable for any loss, actions, claims, proceedings, demand or costs or damages whatsoever or howsoever caused arising directly or indirectly in connection with or arising out of the use of this material.



Microstructural Development of Uniaxial Stretched Anneal-Oriented Syndiotactic Polystyrene and its Blend with Poly (2,6-dimethyl-1,4-phenylene oxide): DSC, WAXD, SAXS and FTIR Studies

Asok Kumar Dikshit

Central Glass and Ceramic Research Institute (CGCRI), Kolkata, India

Studies have been done on strain-induced microstructure development in syndiotactic polystyrene (s-PS) and its blends with poly (2,6-dimethyl-1,4-phenylene oxide) (PPO) in 70/30 and 50/50 compositions of stretched annealed samples. Wide-angle X-ray showed that crystal orientation is less in annealed blend samples compared to annealed pure s-PS for a higher draw ratio. It increases with annealing, and relaxation occurs after a certain annealing temperature at above 180° for both s-PS and s-PS/PPO 70/30 blends. No crystal orientation was observed in the blend of s-PS/PPO 50/50 stretched samples. Small angle X-ray scattering (SAXS) shows the inclusion of amorphous PPO chains in between s-PS crystals lamella. Fourier transform infrared (FTIR) spectroscopy shows that the s-PS molecular chain packing band at 905 cm⁻¹ is enhanced due to annealing in oriented samples and saturates to around 0.63. The

Received 21 December 2009; in final form 7 March 2010.

This research work was supported by the Japan Society for the Promotion of Science (JSPS) research grant PB 01704. A.K. Dikshit is indebted to Dr. A. Kaito for his support to carry out this research work at the National Institute of Advanced Industrial Science and Technology (AIST), Tsukuba Science City, Japan.

Address correspondence to Asok Kumar Dikshit, Central Glass and Ceramic Research Institute (CGCRI), 196, Raja S.C. Mullick Road, Kolkata 700032, India. E-mail: akd@cgcri.res.in

crystal chain relaxation is lower than amorphous chains of s-PS. The molecular chains of amorphous PPO are less oriented into the blend matrix, whereas its relaxation is enhanced during heat treatment and reaches an optimum value after full relaxation. The different behaviors of orientation and relaxation of s-PS and PPO chains into the blend matrix produce superstructures.

Keywords annealing, blends, orientation relaxation, poly(2,6-dimethyl-1,4-phenylene oxide), syndiotactic polystyrene

INTRODUCTION

Syndiotactic polystyrene (s-PS) is a potential commercial polymer because of its excellent thermal, dimensional, and moisture absorption properties and complex polymorphism behaviors compared to other polyolefines. There are four kinds of crystalline modifications (α , β , γ , and δ) and two different mesomorphic forms observed for s-PS. The α and β forms are trans-zigzag planar conformation (T_4), whereas (γ and δ) are all trans trans-gauche gauche (T_2G_2) helical conformation. The α -form crystal structure is hexagonal and the β -form is orthorhombic in nature. The forms of α and β are again subdivided into another two limited disorder forms (α' and β') and limited order forms (α'' and β'') respectively [1–7].

Polymer blends have gained considerable interest from both scientific and commercial points of view, because both components in the blends are combined to give the useful properties of individual components. The polymorphism of s-PS is altered due to blending with another polymer from a more stable trans-zigzag planar (α) to a trans trans -gauche gauche (T_2G_2) helical β -form, and subsequent processing by molecular orientation will produce a new superstructure through structure development. It is important to consider the structure development of syndiotactic polystyrene (s-PS) and its blends with PPO in a molecular-oriented state through annealing [8–10]. Molecular orientation plays a key role to develop a structure. Basically two different molecules in the blend components orient in two different ways in the blend matrix to produce a new superstructure. The effect of blending on annealing with syndiotactic polystyrene (s-PS) in their crystal structure, molecular orientation, and polymorphism is also important.

The commercial importance of s-PS is control through crystallization under different processing conditions involving stretching and subsequent annealing. It was observed that crystallites of s-PS had spherulite morphology. Both spherulite growth rate and overall rate of crystallization were influenced on the method of sample preparation as well as crystallization temperature [11].

Prud'home et al. [12] studied the molecular orientation and relaxation of polystyrene/poly (2,6-dimethyl-1,4-phenylene oxide)(PS/PPO) miscible blends

at above T_g during and after a rapid uniaxial deformation. They showed that both the PS and PPO chain orientation functions increase with stretching rate and PPO content, whereas they decrease with temperature. They also observed that the much higher orientation of PPO in the blends with a PS matrix is due to the higher entanglement density of isolated PPO chains compared to PS chains. Monnerie et al. [13–15] studied the PS-PPO blend system and showed that the PS matrix and PPO oriented in a different manner into the blend system due to interchain interaction during stretching. The chain orientation of PS and PPO decreases with an increase in PS chain relaxation, and the interaction prevents local chain segment motion of PS chains. Cakmak et al. [16] has reported the uniaxial drawing behaviors of the PEEK/PEI blend system. They showed that during uniaxial deformation, a highly physical network structure was formed when oriented crystallites act as nodes in the network structure. The crystalline domain increases very rapidly with drawing, the tie knot of chains are aligned in the drawing direction and the network structures form into crystallites. The molecular chain orientation is enhanced due to blending with PEI.

The previous paper reported on the structure and mechanical properties of highly oriented films of syndiotactic polystyrene and poly (2,6-dimethyl phenylene 1,4-oxide) (s-PS/PPO) miscible blends, where the amount of mesophase and molecular orientation was analyzed. The mesophase content increases with the draw ratio but it saturates after a draw ratio of 3. The amount of mesophase decreases with increasing PPO content for the same draw ratio. But the improved mechanical properties of s-PS/PPO blends in a vertical direction remain the same as those with s-PS in a parallel direction. These effects were explained to relate with the relaxation of amorphous orientation and the synergetic effect for the blend system [2].

Here we will report on the role of uniaxial deformation and the subsequent annealing of syndiotactic polystyrene (s-PS) and poly (2,6,-dimethyl-1,4 phenylene oxide) (PPO) blends on structural development. These studies are essential to obtain information about high-performance polymer materials of s-PS-PPO blends for use-oriented application in commercial fields. The thermal study was done by DSC, and structural information by wide-angle X-ray diffraction (WAXD), and small-angle X-ray diffraction (SAXD). The behavior of polymer chain orientation of s-PS and PPO were done by polarized FTIR spectroscopy.

EXPERIMENTAL

Sample Preparation

The samples used in this study were syndiotactic polystyrene (s-PS) > 90% syndiotacticity) with weight average and number average molecular weights,

$M_w = 2,09,000$ and $M_n = 78,000$, respectively; and poly(2,6-dimethyl-1,4-phenylene oxide) (PPO) with $M_w = 50,000$ and polydispersity of 1.9. The samples s-PS and PPO were purchased from Scientific Polymer Products, Inc. The s-PS/PPO blends with molar ratio 70/30 and 50/50 were prepared by casting chlorobenzene solution with a concentration of (0.4–0.6) wt%. The films were dried at 80°C under vacuum for 2 days to remove the solvent. The films were then melt-quenched in ice water at 0°C after hot pressing at 300°C to obtain amorphous blend films. The amorphous films of pure s-PS were prepared by quenching the molten films in the same ways for the blend films. The samples were stretched in different draw ratios using a hand-operated stretching instrument at a moderate rate in an air-circulating environmental cabinet at controlled temperatures within an accuracy of $\pm 1.5^\circ\text{C}$. The drawing temperature was optimized at 105, 130, and 150°C for pure s-PS, s-PS/PPO 70/30, and s-PS/PPO 50/50 blends, respectively. The drawing temperatures are higher than the glass transition temperature of the three samples by a similar degree (5–10°C) in every case. The samples can be drawn to a higher draw ratio at higher drawing temperatures, but orientation is significantly relaxed. On the other hand, it is difficult to stretch the samples at lower temperatures than the drawing temperature studied in this work. The difference in the drawing temperature was not thought to affect the orientation or the crystal modifications significantly because the drawing temperature was higher than the glass transition temperature by a similar degree ($\sim 10^\circ\text{C}$) in the three experiments. The drawn samples were heat-treated at a constant length at the desired temperature in a temperature-controlled vacuum oven for 24 h.

Characterization

Differential scanning calorimetry (DSC) was measured under nitrogen flow at a heating rate of 10 K/min with a PerkinElmer DSC-7 differential scanning calorimeter calibrated with indium and zinc. The wide-angle X-ray diffraction (WAXD) patterns were measured with the imaging plates (IP) using monochromatized CuK_α radiation with a wavelength of 0.1542 nm (40 KV and 200 mA) generated by a Rint 2500 VH/PC X-ray diffractometer (Rigaku Co., Ltd.). The WAXD profiles were obtained from the imaging plates (IP) of digitized data using the imaging plate reader (Rigaku Raxis DS). Small-angle X-ray scattering (SAXS) patterns were obtained by microfocused CuK_α radiation (45 KV, 60 mA) generated by X-ray diffractometer (Rigaku, Ultrax 4153A 172B). The SAXS profiles were obtained from the imaging plate detector from the imaging plates of digitized data. The polarized FTIR spectra were recorded at a resolution of 4 cm^{-1} with a BioRad FTS 60A-686 FTIR spectrophotometer (Bio-Rad, Hercules, CA)

equipped with a wire-grid polarizer. The dichroic ratio was calculated from the ratio of intensities of a particular band for parallel as well as perpendicular directions.

RESULTS AND DISCUSSION

Thermal Properties

Figure 1 shows the DSC thermograms of pure s-PS, pure PPO and the s-PS/PPO blends with compositions of s-PS/PPO = 70/30, 50/50, and 30/70. All are obtained by quenching the melts to ice water at 0°C. The glass transition temperature, T_g , of pure s-PS and PPO are 98 and 210°C, respectively. The crystallization (T_c) and melting peaks (T_m) are observed at 144 and 268°C, respectively, in the DSC curve of pure s-PS. The enthalpy change (ΔH_c) during crystallization is in good agreement with the enthalpy change, (ΔH_m) during melting, and henceforth the melt quenched s-PS is amorphous in nature as well as the other quenched samples. A single glass transition is observed for each blend sample, suggesting that the s-PS/PPO system is miscible in the amorphous phase. T_g shifts toward the higher temperature with an increase in PPO content.

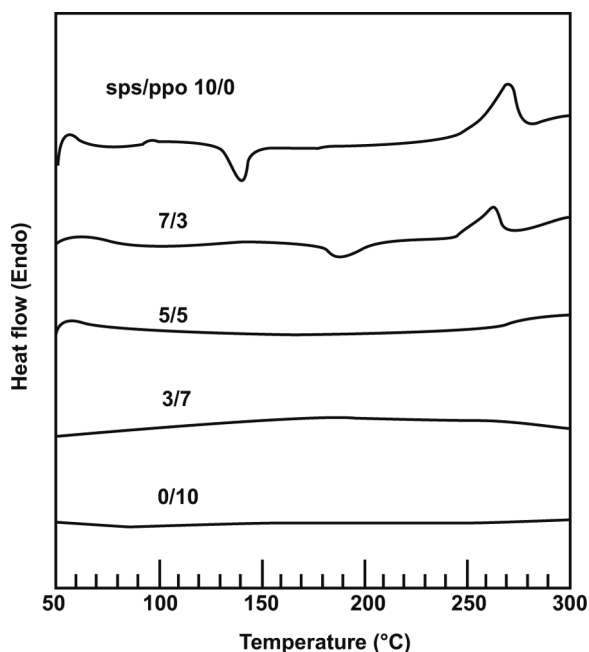


Figure 1: DSC thermograms of melt-quenched samples of s-PS, PPO, and s-PS/PPO blends with compositions of s-PS/PPO = 70/30, 50/50, and 30/70.

WAXD Results

Figure 2 shows highly drawn oriented mesophase structural morphology of pure s-PS (Figure 2a), s-PS/PPO 70/30 (Figure 2b), and s-PS/PPO 50/50 (Figure 2c) blends of draw ratio 6, annealed at 240, 240 and 200°C, respectively, for 24 h. The diagrams represent the six-point pattern consisting of an equatorial reflection at $2\theta = 12.2^\circ$ and a diagonal reflection at $2\theta = 20.4^\circ$, which are attributed to the mesomorphic phase of s-PS [11–14]. The amount of mesophase in nonannealed samples for pure drawn s-PS and its blends has been discussed in an earlier publication [2]. It has been observed that samples are more oriented. They are annealed at 240°C compared to blend samples where orientation relaxed and crystallization spots in diffraction are more intensified. When samples are annealed at 240°C, it was observed that orientation relaxation and crystallization spots in diffraction are more intensified for blended samples. It can be explained that during uniaxial deformation of polymer chain, the s-PS chains are oriented in a stretching direction. They are able to make some multichain junction cross points which are more aligned during heat treatment. These cross points of multichain junction act as tie knots [16].

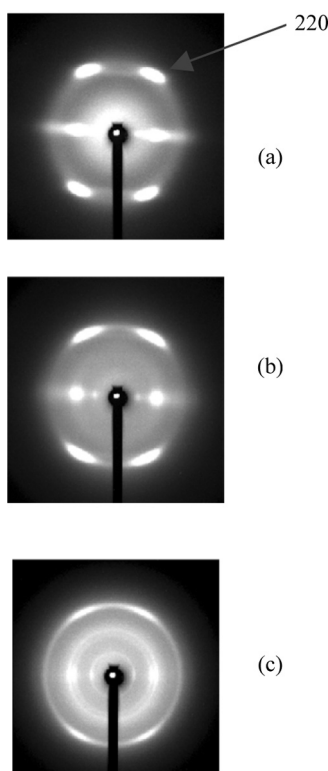


Figure 2: WAXD diagram of annealed samples of draw ratio 6: (a) s-PS; (b) s-PS/PPO = 70/30 and (c) s-PS/PPO = 50/50.

Auriemma et al. [17] analyzed the mesomorphic form of s-PS, a simulation of the X-ray diffraction intensity-based model consisting of s-PS chain bundles with paracrystalline disorder. Since the crystal orientation is markedly relaxed and crystal reflections are sharper in the s-PS/PPO 50/50 blend, it could have been explained that molecular chains are mobile enough to relax the molecular orientation in the blend sample during thermal treatment due to high entropy higher order state to low entropy relaxed state. The observed crystal spots in the WAXD diagrams are responsible for α' crystalline form of s-PS. But in the s-PS/PPO 70/30 blend (Figure 2b) sample the α' crystalline form is more intensified and a small amount of β' form and considerable amount of α'' are induced by thermal treatment. The s-PS crystal orientation is less in the s-PS/PPO 70/30 blend. In the annealed WAXD diagrams shown Figure 2(c), crystal reflections are resolved, and spots are a mixture of α' and β' crystal of s-PS. There was no orientation observed since PPO content is more in this blend which is responsible for relaxation of s-PS crystal under thermal treatment. The reflections of the different polymorph of s-PS crystals has been summarized in Table 1 [2]. The observed reflections at 220, 310, 400, 320, 410, and 210 are formed of α'' -crystal, whereas only 220 are formed of α' -crystal.

Figure 3 shows a WAXD diagram of s-PS of draw ratio 4 annealed at different temperatures (a) 160°; (b) 180°; (c) 200°; (d) 220° and (e) 240°C, respectively, for 24 h. It has been observed that the crystal orientation increases with annealing from 160 to 180°C as 220 spot width increases initially, whereas it relaxes after annealing on and above 180°C. The observed WAXD spots are at $2\theta = 6.7, 11.8, \text{ and } 13.5^\circ$ which correspond to the α' -crystalline form of s-PS. It is reported that α' -crystalline forms are obscured by the mesophase reflection at a lower crystallization temperature ($<180^\circ\text{C}$), whereas the α'' -form reflections are resolved from the mesophase scattering only at higher crystallization temperatures ($>200^\circ\text{C}$). The initially enhanced crystal orientation during annealing at 160 to 180°C could be explained due to the fact that stretched samples are more orderly. They start relaxation after annealing at

Table 1: WAXD data for different modified s-PS crystals (2).

α' -Crystal		α'' -Crystal		β' -Crystal	
2θ	hkl	2θ	hkl	2θ	hkl
6.7	110	6.7	110	6.1	020
		10.3	210	10.4	110
11.8	300	11.7	300	12.3	040
13.5	220	13.5	220	13.6	130
		14.0	310		
		15.6	400		
		17.1	320		
		18.0	410	18.6	150/060
20.3	211	20.3	211	20.2	111

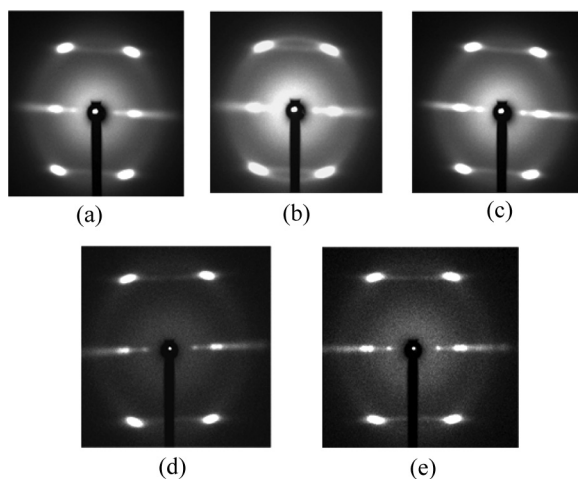


Figure 3: WAXD diagram of annealed s-PS of draw ratio 4 at different temperatures (a) 160°C; (b) 180°C; (c) 200°C; (d) 220°C and (e) 240°C.

200°C onwards, because high temperature is a source of much more thermal energy, which is responsible for higher entropy that tends to lower entropy by relaxation phenomena. This information is similar to previous reported results [11–18]. The oriented α' -form crystals of s-PS films are more disordered compared to those in the isotropic films of s-PS.

Figure 4 shows a WAXD diagram of annealed s-PS/PPO 70/30 of draw ratio 4, at different temperatures: (a) 160; (b) 180; (c) 200; (d) 220 and (e) 240°C. These diagrams reveal that α' -form reflections were dominant in pure s-PS and are well-resolved in this blend. This suggests that α' -form crystals in these

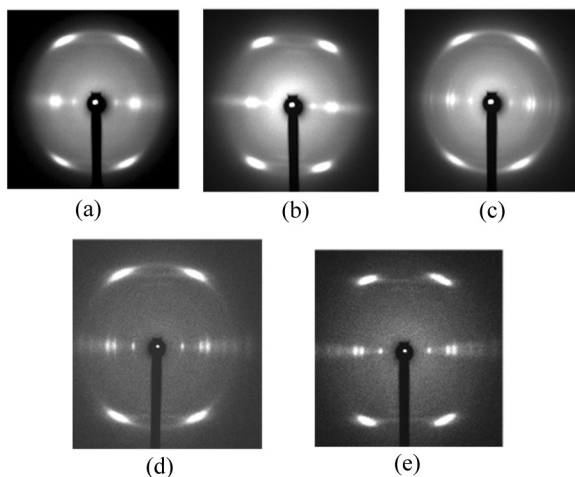


Figure 4: WAXD diagram of annealed s-PS/PPO 70/30 of draw ratio 4 at different temperatures (a) 160°C; (b) 180°C; (c) 200°C; (d) 220°C and (e) 240°C.

s-PS/PPO 70/30 blend films are more ordered, even larger than drawn annealed s-PS films. For annealing at 180°C and above, samples observed new crystal spots. A small amount of β' form is produced when crystallized at (180–200)°C, but a considerable amount of α' -form is generated in the s-PS/PPO 70/30 blend when annealed at higher temperatures (>200°C) [11]. WAXD diagrams showed that crystal orientation is much less than the pure s-PS as the crystal spot of 220 reflections becomes wider in the s-PS WAXD diagram. The width of s-PS enhances in s-PS/PPO 70/30, when annealed at 160 to 180°C; but it again decreases from 180 to 200, 220 and 240°C, respectively. This is due to more orderly crystals in the stretching direction. This enhances crystal orientation under thermal force, but after certain ordering of the crystal, they are relaxed at temperatures above 160°C. The relaxation of s-PS crystal orientation in the s-PS/PPO 70/30 blend increases with the increase in annealing temperature. It can be explained that polymer chains of amorphous PPO chains are more mobile and soft in the blend matrix, which relaxes from high entropy unstable strain state to low entropy stable state under thermal driving force.

Figure 5(a–e) shows WAXD diagrams of annealed s-PS/PPO 50/50 of draw ratio 4 at different temperatures (a) 160; (b) 180; (c) 200; (d) 220

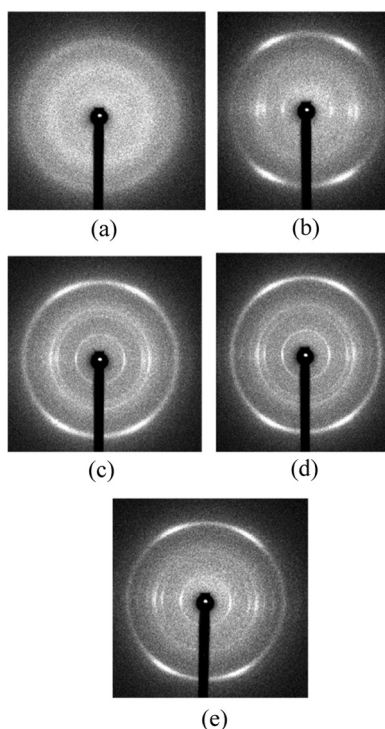


Figure 5: WAXD diagram of annealed s-PS/PPO 50/50 of draw ratio 4 at different temperatures (a) 160°C; (b) 180°C; (c) 200°C; (d) 220°C and (e) 240°C.

and (e) 240°C, respectively. Here, no crystal orientation and crystal reflections are observed up to an anneal temperature at 160°C, where crystal reflections are sharper at 180°C and above. It is assumed that slippage of polymer chains in the presence of diluents PPO are responsible for the relaxation of crystal orientation and crystal reflections. They are more prominent and sharper in s-PS/PPO 5/5 blends. In our previous paper, it was reported that α' and β' forms are observed after annealing at 180°C, and the intensities of the α'' -form peaks increase with the crystallization temperature increases. The sharp reflections are observed at 240°C crystallization of s-PS/PPO 50/50 blends. The 211 reflection of the α' and α'' -forms is intensified with increasing crystallization temperature due to relaxation of the crystal orientation. So, it is considered that the crystalline order of the α' and α'' forms increases with PPO content. Generally it was observed that the crystal reflection becomes narrow with an increase in diluent content in a crystalline/amorphous blend, but here we observe the reverse for the s-PS/PPO system.

SAXS Results

Figure 6(a–c) shows a SAXS diagram of draw ratio 6 (a) s-PS anneal at 240°C; (b) s-PS/PPO 70/30 and (c) s-PS/PPO 70/30 annealed at 240°C; the longitudinal meridian scattering lobe streaks in Figure 6(a) are for microvoid

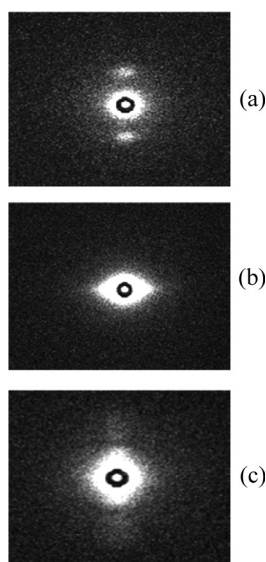


Figure 6: SAXS diagram of draw ratio 6 (a) s-PS; (b) s-PS/PPO 70/30 and (c) s-PS/PPO 70/30 anneal at 240°C.

diffraction and stacks of lamella diffraction of s-PS, which is induced during stretching and annealing. It was important to observe that the direction of the small angle diffraction streak is changed from equatorial to longitudinal in a nonannealed to annealed, highly drawn blend sample of s-PS/PPO 70/30 (Figure 6(b–c)). The equatorial streak is due to bundles of micro fibrils diffraction, which is originated from the induction of stretching initial spherulites of s-PS crystal deformed into lamellae, which are again transformed into micro fibrils upon further orientation by thermal driving force during annealing towards the stretching direction [19]. The highly drawn annealed s-PS/PPO 70/30 blend sample has narrow stacks of lamellae alternating crystalline s-PS and noncrystalline layers of PPO, where PPO molecular chains are included between two s-PS crystalline lamellae.

The Lorentz-corrected SAXS profiles of the anneal (a) s-PS, (b) s-PS/PPO 70/30 and (c) anneal s-PS/PPO 70/30 of draw ratio 6 is shown in Figure 7. The apparent scattering peaks are at low q position. The scattering intensity inflection peak is in higher q shifted in the blend 70/30 annealed sample. This is because of reorganization and crystallization into the structure of shorter periods. It can be explained that diffusion of amorphous chains of PPO into the interlamellar s-PS region causes decrease of lamella thickness in the blend annealed sample. It shows that annealed drawn s-PS and annealed drawn s-PS/PPO 70/30 exhibits weak scattering at 0.62 nm^{-1} and 0.8 nm^{-1} , corresponding to long periods where $L = 10 \text{ nm}$ and $L = 8 \text{ nm}$, respectively. The interlamellar morphology calculation was done using the Lorentz-corrected

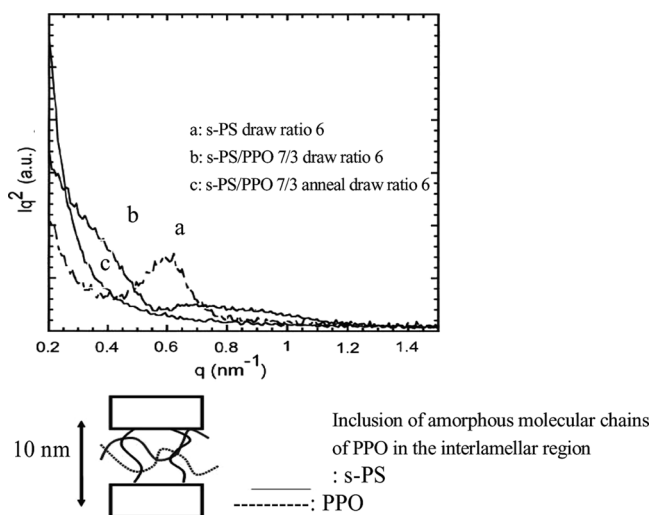


Figure 7: Lorentz-corrected SAXS profile of oriented samples in meridional direction for draw ratio 6 (a) anneal s-PS; (b) s-PS/PPO 70/30 and (c) anneal s-PS/PPO 70/30.

relation $L = 2\pi/q_m$, where q_m is the average of the long period which is the sum of the crystalline and amorphous components in the structure.

FTIR Studies

Figure 8(a–c) shows polarized FTIR spectra of draw ratio 6 from 400 cm^{-1} to 1400 cm^{-1} for pure s-PS, s-PS/PPO 70/30 and s-PS/PPO 50/50 blend films, respectively. The s-PS and PPO band spectra at above 1400 cm^{-1} are overlapping each other, whereas the absorption bands of the two components are separated from each other in the wave number region below 1400 cm^{-1} . The absorption bands in this region ($400\text{--}1400\text{ cm}^{-1}$) show large dichroism, suggesting that the molecular chains of s-PS and PPO both are highly oriented before annealing. PPO shows absorption bands [2,8,11,12,14,16,18,20–23] at

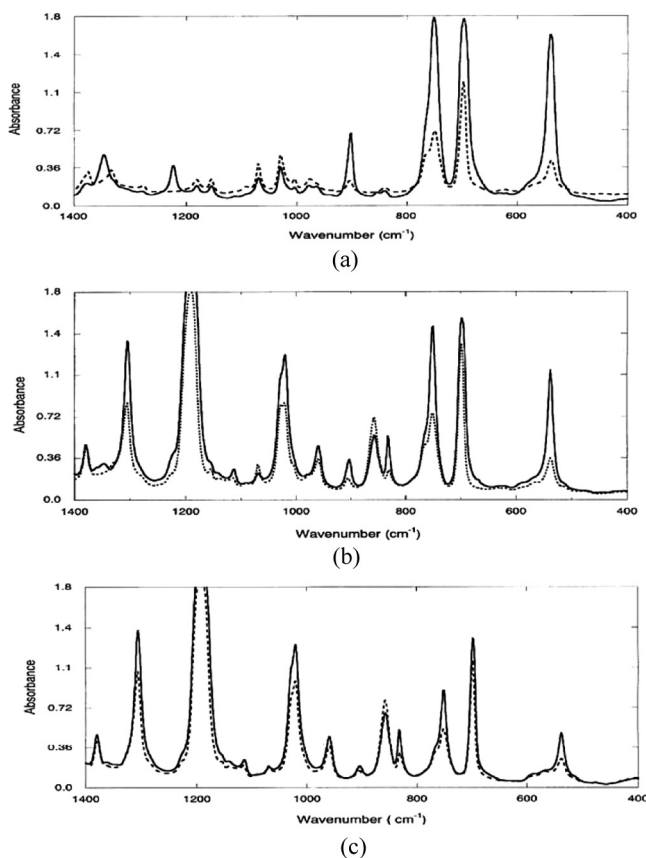


Figure 8: Polarized FTIR spectra of a drawn film of s-PS with a draw ratio of 6 in the wave number region of $400\text{--}1400\text{ cm}^{-1}$; (a) s-PS; (b) s-PS/PPO = 7/3; (c) s-PS/PPO = 5/5; (-) parallel polarization; (- -) perpendicular polarization.

1305, 1190, 1021, 960, 858, and 832 cm^{-1} , whereas s-PS shows absorption bands at 1375, 1334, 1278, 1222, 1182, 1155, 1069, 1029, 1004, 977, 903.5, 840, 751, 698 and 539 cm^{-1} . The orientation functions (F) were measured from the following equation:

$$F = (D - 1)/(D + 2) \quad (1)$$

where D is dichroic ratio, it was obtained from the ratio of the integrated area of intensity of absorption bands in parallel and perpendicular directions with respect to the chain axis ($D = A_{\text{Parallel}}/A_{\text{Perpendicular}}$) [3]. We already reported that the orientation of the polymer chain does not change significantly with a lower draw ratio by the composition and heat treatment.

Figure 9 shows orientation function vs. various annealing temperatures of draw ratio 4, of the PPO band of 858 cm^{-1} and 832 cm^{-1} . The amount of mesophase is of the same order of magnitude for a draw ratio of 4 and draw ratio of 6 samples. Henceforth, the samples of draw ratio 4 have been chosen for thermal treatment study to avoid shrinkage [2]. The sample thickness was less than 25 micron for FTIR measurements. The 960 cm^{-1} peak is for PPO, which is oriented in room temperature with a value of about 0.24. It relaxes gradually on high temperature annealing. The 858 cm^{-1} band is originating from out of plane bending vibration of the 1,2,4,6-tetrasubstituted benzene ring of PPO. It is a perpendicular sensitive band and henceforth a negative value is observed [11,16,24]. The orientation function of this band is -0.17 at a stretching temperature of 130°C . It reaches zero after annealing at a

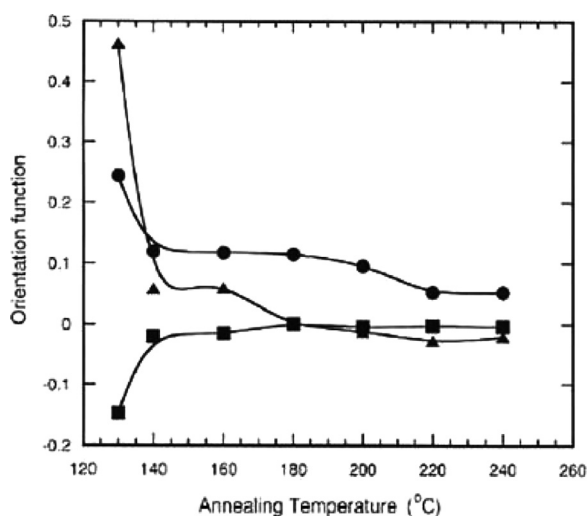


Figure 9: Orientation functions vs. annealing temperatures of (●), 960 cm^{-1} , (▲), 832 cm^{-1} and (■), 858 cm^{-1} bands.

temperature greater than 130°C. On the other hand, the orientation of the parallel sensitive amorphous PPO band at 832 cm⁻¹ is 0.48 at room temperature. The chain orientation decreases with temperature and reaches zero at 180°C. This band originates from the -CCH bond vibration of PPO. These chain orientation relaxations due to temperature can be explained as these are in the amorphous PPO band. It is very soft and mobile in the blend matrix. The chain orientation relaxes through annealing due to the stretching-induced strain of the PPO chain under the thermal driving force.

The orientation function of the amorphous chains of PPO was measured from the dichroic ratio of the 858 cm⁻¹ band. It decreases with parallel alignment of the molecular chains into the draw direction. The transition moment vector of this band is perpendicular to the polymer chain axis [24]. The degree of orientation of molecular chains increases with increasing draw ratio in the nonannealed drawn samples. It is relaxed in annealed samples. This is due to the fact that the stiffer polymer chain PPO can't be relaxed during the stretching period, but it can during heat treatment for movement from a high entropy strain system to a low entropy stable system.

Figure 10 shows the orientation function vs. annealing temperature of s-PS band [25] of 903.5 cm⁻¹, which is originated from the packing of the s-PS polymer chain during annealing of oriented s-PS, where the structural organization and crystallization occurs. This is the conformational insensitive band of s-PS, and it is generally observed in the amorphous sample at 905 cm⁻¹. This is shifted to 902 cm⁻¹ in the α -form of trigonal to 911 cm⁻¹ in

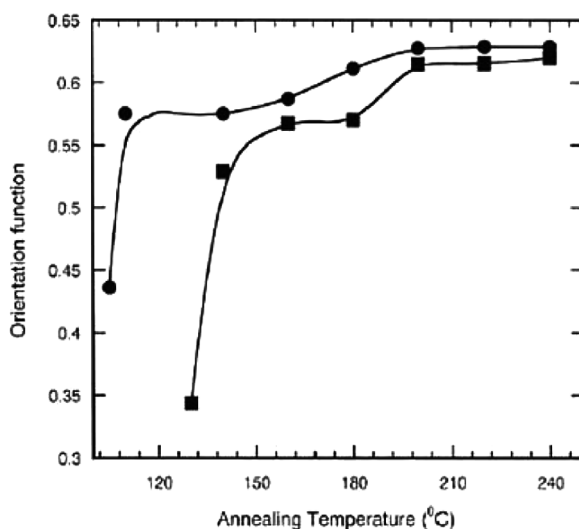


Figure 10: Orientation function vs. annealing temperatures of 905 cm⁻¹ band; (●), s-PS; and (■), s-PS/PPO 70/30.

the β -form of orthorhombic. It is important to note that orientation increases markedly in both a pure s-PS and s-PS/PPO 70/30 blend initially with an increase of annealing temperature. It reaches a constant value after annealing at 200°C. Generally, it is observed that polymer chain orientations are relaxed during heating, as strain-induced high entropy occurs during stretching. It can be explained that the initial orientation of the polymer chain in itself and in blends is more oriented by reorganization in uniaxial stretch direction during annealing. The orientation reaches saturation when the temperature is high, as limiting chains are fully oriented in the stretching direction. The orientation is less in 70/30 blends compared to pure s-PS since polymer chains are more mobile and soft into blend matrix. Henceforth, the relaxation effect is marked in blended samples. It is noted that the initial packing of crystal in the chain is prominent in both pure s-PS and also s-PS/PPO 70/30 blends from room temperature. The chain orientation is markedly enhanced in the blend compared to pure s-PS. The final reorganization of polymer chain packing of the crystal become optimum at 200°C. The orientation of the 903.5 cm^{-1} band of the s-PS polymer chain increases with draw ratio, whereas it decreases with PPO composition before annealing. It enhances on annealing in both pure s-PS as well as in blend samples due to more packing of s-PS polymer chains during heat treatment.

Figure 11 shows orientation function vs. various annealing temperature of draw ratio 4 of s-PS bands at 1069 cm^{-1} . This band is originating from a ring in plane CCH bending vibration for both all-trans and helical conformation

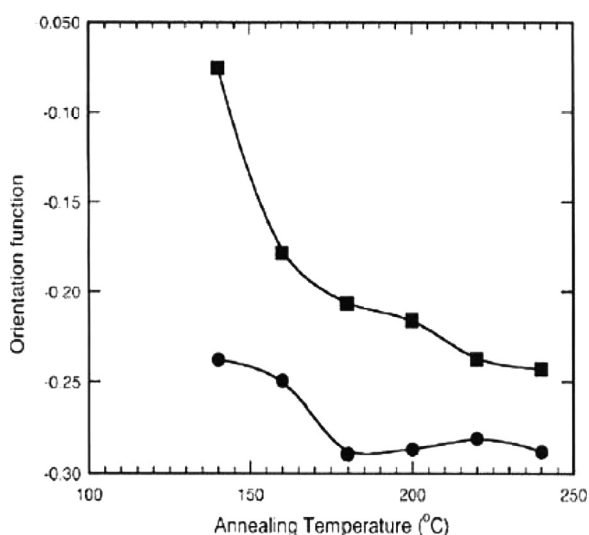


Figure 11: Orientation function vs. annealing temperatures of 1069 cm^{-1} band; (●), s-PS; and (■), s-PS/PPO 70/30.

and insensitive to conformation [16,24–27]. It is the s-PS conformation perpendicular sensitive band. The s-PS chain orientation sharply increases on thermal treatment due to more order and the compactness of the s-PS polymer chain towards the stretching direction. It reaches saturation at higher temperature due to full conversion of all chains in the stretching direction. The s-PS/PPO 70/30 blend is less oriented, whereas the same trend is also observed in a pure s-PS drawn sample. The poor orientation of the blended sample can be explained due to higher mobility and softness of the s-PS polymer chain in the blend matrix, which is responsible for the relaxation of the polymer chain under thermal potential.

Figure 12 shows orientation function vs. annealing temperatures at 1305 and 1378.5 cm^{-1} band in s-PS/PPO 70/30 blends; these are employed for structural analysis of PPO, because other small bands are overlapping with absorption bands of s-PS. Henceforth, it is difficult to assign structural features of PPO using other bands. 1305 cm^{-1} is a negative sensitive transition moment vector band relative to the chain axis, whereas the 1378.5 cm^{-1} band is a positive sensitive transition [16,24–27]. The PPO chain orientation is gradually relaxed in s-PS/PPO 70/30 blends as shown in Figure 12 during heat treatment in both the 1305 cm^{-1} and 1378.5 cm^{-1} band. As PPO chains are amorphous and very soft in nature, so orientation becomes easily relaxed due to external heat treatment. It has been observed that PPO chain orientation relaxation is very prominent at 130–170°C and relaxes to an optimum for both 1305 cm^{-1} and 1378.5 cm^{-1} band.

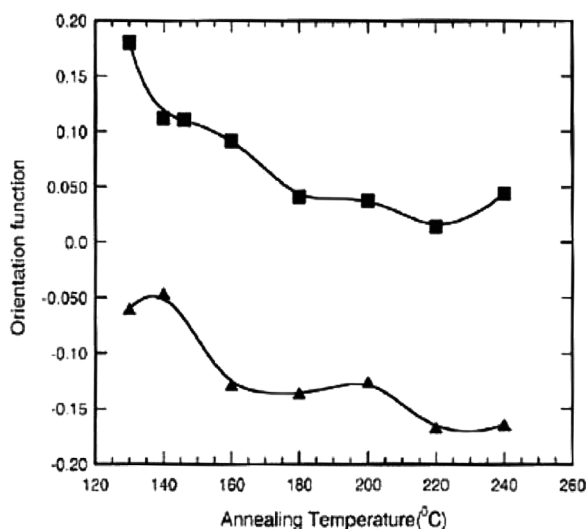


Figure 12: Orientation function vs. annealing temperatures of (■), 1305 cm^{-1} and (▲), 1378.5 cm^{-1} bands of PPO.

CONCLUSIONS

The orientation and microstructural development in uniaxial stretched s-PS and s-PS/PPO 70/30 and 50/50 blends have been analyzed as a function of annealing temperature and also for different blend compositions. The orientation relaxation is more enhanced in blend samples compared to pure stretched s-PS samples. The s-PS crystal relaxes and a sharper crystal reflection is observed in blend samples compared to that in pure s-PS. The mobility of PPO molecular chains is more than s-PS molecular chains with annealing temperature. The PPO chains are included between s-PS crystal lamellae into the blend matrix. The molecular chains of s-PS are more compact and orderly during annealing in both s-PS and blends matrix. PPO bands are also oriented during stretching, whereas it relaxes by heat treatment with the formation of microstructure.

REFERENCES

- [1] Liu, C. K., Nguyen, T., Yang, T.-J., and Lee, S. *Polymer* **50**, 499 (2009).
- [2] Dikshit, A. K., and Kaito, A. *J. Polym. Sci. B: Polym. Phys.* **41**, 1665 (2003).
- [3] Dikshit, A. K., and Kaito, A. *J. Appl. Polym. Sci.* **91**, 2789 (2004).
- [4] Rosa, C. De., Rizzo, P., Ballesteros, O. R., Petraccone, V., and Guerra, G. *Polymer* **40**, 2103 (1999).
- [5] Kimura, T., Ezura, H., Tanaka, S., and Ito, E. *J. Polymer Sci. B: Polymer Physics* **36**, 1227 (1998).
- [6] Kobayashi, M., Nakaoki, T., and Ishihara, N. *Macromolecules* **23**, 78 (1990).
- [7] Kobayashi, M., Tsumura, K., and Tadokoro, H. *J. Polym. Sci. Polym. Phys. Ed.* **6**, 1493 (1968).
- [8] Sun, Y. S., and Woo, E. M. *J. Polym. Sci. B: Polymer Physics* **40**, 176 (2002).
- [9] Sun, S., and Woo, E. M. *J. Polym. Sci. B: Polymer Physics* **38**, 3210 (2000).
- [10] Woo, E. M., and Wu, F. S. *Macromol. Chem. Phys.* **199**, 2041 (1998).
- [11] Yan, R. J., Aji, A., Shinozaki, D. M., and Dumoulin, M. M. *Polymer* **41**, 1077 (2000).
- [12] Zhao, Y., Keroack, D., and Prud'home, R. *Macromolecules* **32**, 1218 (1999).
- [13] Lefebvre, D., Jasse, B., and Monnerie, L. *Polymer* **22**, 1616 (1981).
- [14] Lefebvre, D., Jasse, B., and Monnerie, L. *Polymer* **25**, 318 (1984).
- [15] Halary, J. L., Creton, L., and Monnerie, L. *Polymer* **40**, 199 (1999).
- [16] Bicakci, S., and Cakmak, M. *Polymer* **43**, 2737 (2002).
- [17] Auriemma, F., Petraccone, V., Poggetto, F. D., Rosa, C. De., Guerra, G., Manfredi, C., and Corradini, P. *Macromolecules* **26**, 3772 (1993).
- [18] Guerra, G., Rosa, C. De., Vitagliano, V. M., Petraccone, V., and Karaz, F. E. *Polymer Communication* **32**, 30 (1991).
- [19] Wenig, W., Karasz, F. E., and MacKnight, W. J. *J. Appl. Phys.* **46**, 4194 (1975).

- [20] Guerra, G., Vitagliano, V. M., Rosa, C. De., Petraccone, V., and Corradini, P. *Macromolecules* **23**, 1539 (1990).
- [21] Guerra, G., De Rosa, C., Vitagliano, V. M., Petraccone, V., and Corradini, P. *J. Polym. Sci. B: Polymer Physics* **29**, 265 (1991).
- [22] Vasanthan, N., Corrigan, J. P., and Woodward, A. E. *Polymer* **34**, 2270 (1993).
- [23] Musto, P., Tavone, S., Guerra, G., and De Rosa, C. *J. Polym. Sci. B: Polym. Phys.* **35**, 1055 (1997).
- [24] Messe, L., and Prud'home, R. E. *J. Polymer Sci. B: Polymer Physics* **38**, 1405 (2000).
- [25] Painter, C. P., and Koenig, J. L. *J. Polym. Sci. Polym. Phys. Ed.* **15**, 1885 (1977).
- [26] Mastuba, G., Kaji, K., Nishida, K., Kanaya, T., and Imai, M. *Macromolecules* **32**, 8932 (1999).
- [27] Benedetti, E., Moscatelli, D., and Vergamini, P. *Macromol. Chem. Phys.* **203**, 1497 (2002).